

Detection of abundant solid methanol toward young low mass stars[★]

K. M. Pontoppidan¹, E. Dartois², E. F. van Dishoeck¹, W.-F. Thi³, and L. d’Hendecourt²

¹ Leiden Observatory, PO Box 9513, 2300 RA Leiden, The Netherlands

² Institut d’Astrophysique Spatiale, Bât. 121, CNRS UMR8617, Université Paris XI, 91405 Orsay Cedex, France

³ Astronomical Institute “Anton Pannekoek”, University of Amsterdam, Kruislaan 403, 1098 SJ Amsterdam, The Netherlands

Received 2 April 2003 / Accepted 24 April 2003

Abstract. We present detections of the absorption band at $3.53 \mu\text{m}$ due to solid methanol toward three low-mass young stellar objects located in the Serpens and Chameleon molecular cloud complexes. The sources were observed as part of a large spectroscopic survey of ≈ 40 protostars. This is the first detection of solid methanol in the vicinity of low mass ($M \lesssim 1 M_{\odot}$) young stars and shows that the formation of methanol does not depend on the proximity of massive young stars. The abundances of solid methanol compared to water ice for the three sources are in the range 15–25% which is comparable to those for the most methanol-rich massive sources known. The presence of abundant methanol in the circumstellar environment of some low mass young stars has important consequences for the formation scenarios of methanol and more complex organic species near young solar-type stars.

Key words. astrochemistry – circumstellar matter – dust, extinction – ISM: molecules – infrared: ISM

1. Introduction

The presence and origin of complex organic molecules in protostellar regions and their possible incorporation in protoplanetary disks is an active topic of research, both observationally and through laboratory simulations. Large organic molecules such as CH_3OCH_3 and $\text{CH}_2\text{CH}_3\text{CN}$ have been detected with enhanced abundances in so-called “hot cores” around massive young stars (e.g. Hatchell et al. 1998; Gibb 2001). In the laboratory, UV photolysis of ice mixtures of species prepared with interstellar abundances followed by thermal warm-up to 300 K is known to lead to a wealth of complex species such as carboxylic acids and esters (Briggs et al. 1992), hexamethylenetetramine (Bernstein et al. 1995) and prebiotic molecules including amino acids (Munõz Caro et al. 2002; Bernstein et al. 2002). In the ice experiments, methanol is thought to be a key molecule in the production of these complex molecules. Understanding the methanol content of interstellar ice mantles and its variation in different circumstellar environments is therefore essential to test the validity of the basic assumptions that enter the chemical models and experimental approach.

So far, solid methanol has only been detected along lines of sight associated with intermediate- to high-mass protostars, with abundances ranging from 5% up to 30% with respect to the dominant ice mantle component, H_2O (Dartois et al. 1999).

Extensive searches toward low-mass protostars have resulted in typical upper limits of a few % (Chiar et al. 1996; Brooke et al. 1999). In contrast, gas-phase methanol has been found toward both high- and low-mass YSOs with evidence for abundance jumps of factors of 100–1000 in the inner part of the envelope, consistent with ice evaporation (e.g. van der Tak et al. 2000; Schöier et al. 2002; Bachiller et al. 1995). Still, the observed gas-phase column densities of methanol are usually $10\text{--}10^4$ times less than those observed in the solid phase (e.g. Schöier et al. 2002). In hot cores, a rapid high-temperature gas-phase chemistry is triggered by the evaporation of methanol-rich ices, which forms high abundances of large organic molecules for a period of $10^4\text{--}10^5$ yr (e.g. Charnley et al. 1992; Rodgers & Charnley 2001). Understanding the origin of solid CH_3OH and its variation from source to source is a key ingredient for these models.

As part of a large VLT-ISAAC $3\text{--}5 \mu\text{m}$ spectral survey toward young low mass stars we have detected an absorption feature at $3.53 \mu\text{m}$ towards at least three icy sources out of ≈ 40 , which is attributed to solid methanol. Two of the sources are part of the dense cluster of young low-mass stars, SVS 4, located in the Serpens cloud core (Eiroa & Casali 1989). The third source is a more isolated low-mass class I source in the Chameleon I cloud known as Cha INa 2 (Persi et al. 1999). The spectra presented here represent the first detections of solid methanol toward low mass YSOs. The observations and analysis are reported in Sect. 2, whereas the implications for the chemical evolution of circumstellar matter are discussed in Sect. 3.

Send offprint requests to: K. M. Pontoppidan,

e-mail: pontoppi@strw.leidenuniv.nl

[★] Based on observations obtained at the European Southern Observatory, Paranal, Chile, within the observing program 69.C-0441.

2. Observations

2.1. The *L*-band spectra

The observations were performed using the Infrared Spectrometer and Array Camera (ISAAC) mounted on the Very Large Telescope UT1-Antu of the European Southern Observatory at Cerro Paranal. *L*-band spectra were obtained using the low resolution mode and the 0".3 slit resulting in resolving powers of $\lambda/\Delta\lambda = 1200$. SVS 4-5 and SVS 4-9 were observed simultaneously on May 5, 2002. Cha INa 2 was observed on May 6, 2002. All spectra were recorded during good weather conditions. The data were reduced using our own IDL routines, which are described in Pontoppidan et al. (2003). Correction for telluric absorption features was done using the early-type standard stars BS 4773 (B5V) and BS 7348 (B8V) for Cha INa 2 and the SVS 4 sources, respectively. The wavelength calibration was obtained using the telluric absorption features with an estimated accuracy of 0.001 μm . The spectra were flux calibrated using the standard stars with an estimated uncertainty of 15%, mainly due to uncertainties in slit losses.

2.2. Derivation of methanol abundances

The water band profile was obtained by adopting a blackbody continuum fitted to a *K*-band photometric point from the literature and the observed *L*-band spectrum from 4.0 to 4.15 μm as well as the *M*-band spectra, which are discussed in detail in Pontoppidan et al. (2003). The 2.8–4.8 μm spectra are shown in Fig. 1. The accuracy of the *K*-band points are crucial for estimating the column density of the water ice bands. However, the *K*-band fluxes have considerable uncertainties since many young stellar objects are known to be highly variable and the sources may have changed their flux level since the photometric measurement. Indeed, Cha INa 2 is known to vary significantly in the *K*-band (Carpenter et al. 2002) and has apparently continuously brightened with 1.7 mag between March 1996 and April 2000 (Persi et al. 1999; Kenyon & Gómez 2001; Carpenter et al. 2002) to $K = 11.044$. It is found that at least $K = 10.2$ is necessary to fit the continuum defined by the ISAAC *L* and *M*-band spectra, consistent with the assumption that the source has continued to brighten until May 2002 with the same rate. The continua used for deriving the optical depths of the water bands are shown in Fig. 1 along with continua fitted using extreme *K*-band fluxes. For the Serpens sources a conservative estimate of the *K*-band variability is 0.2 mag when comparing with the photometry of Eiroa & Casali (1992). For Cha INa 2 continua using $K = 10$ and $K = 12.75$ are also shown.

A local third order polynomial was used to estimate the continuum around the methanol feature (see Fig. 2). The polynomial was fitted to the points between 3.1 μm and 3.2 μm , and the region between 3.63 μm and 3.70 μm . The confidence in the local continuum for extraction of the methanol profiles is high, partly due to the low order of the polynomial and partly due to the low curvature required for the three spectra. The uncertainty in the derived abundances is thus dominated by the main

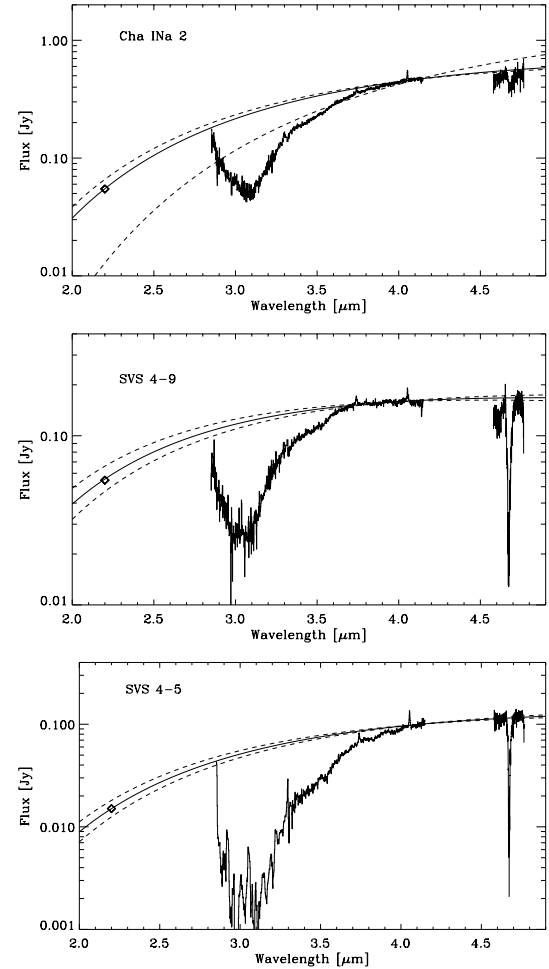


Fig. 1. Adopted blackbody continua for estimating water band optical depths (solid curves). The *K*-band magnitudes (diamonds) for the Serpens sources are taken from Giovannetti et al. (1998). The adopted *K*-band magnitude for Cha INa 2 is discussed in the text. Dashed curves indicate continua calculated using a conservative estimate for the uncertainties on the (sometimes variable) *K*-band fluxes. The spectrum of SVS 4-5 has been smoothed to a resolution of $R = 120$ between 2.8 and 3.3 μm .

water band continuum. The measured water ice abundances are presented in Table 1. The values were derived by fitting a laboratory spectrum of pure amorphous water ice at 50 K to the observed water bands and integrating the scaled laboratory spectrum from 2.5 to 3.7 μm . None of the observed water bands are saturated. However, due to the low S/N ratio in SVS 4-5, the fit in this source relies on the wings in the water band. The adopted band strength is 2.0×10^{-16} cm molec $^{-1}$ (Gerakines et al. 1995). Note that laboratory measurements of solid state band strengths may in general only be accurate within 30%.

The final absorption profiles in the 3.3–3.7 μm region are shown in Fig. 3 on an optical depth scale. Common to the profiles of SVS 4-9 and Cha INa 2 is a broad feature centered at 3.47 μm along with a narrow feature at 3.53 μm seen in all three sources. The former is most likely the same feature seen in this wavelength region toward many other young stars, generally known as the “3.47 μm feature” and thought to be due to diamonds or an ammonia hydrate. The 3.53 μm feature

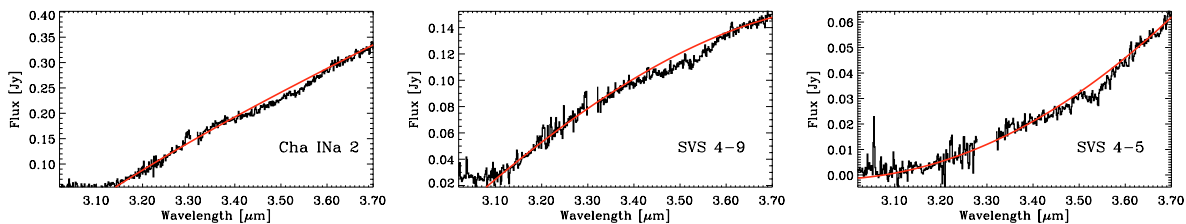


Fig. 2. Local third order polynomial continua for extracting the methanol band profiles.

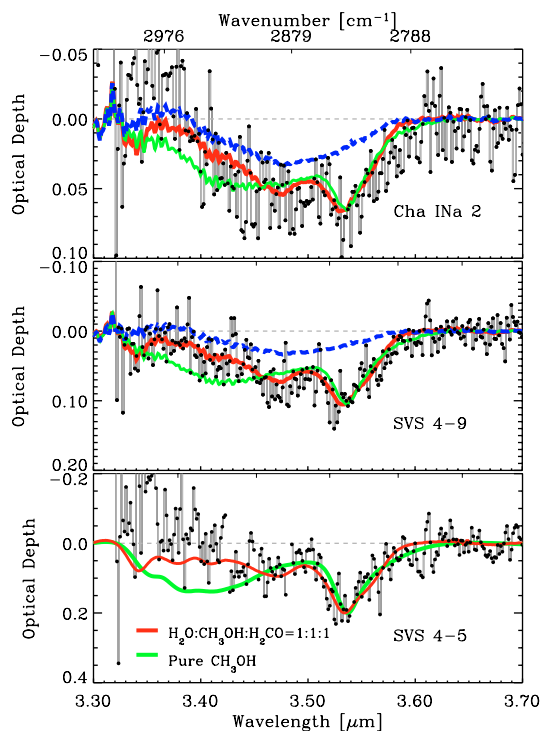


Fig. 3. The detected methanol bands on an optical depth scale. The dashed curve shows the $3.47 \mu\text{m}$ feature from the intermediate mass YSO Reipurth 50. The solid curves show the sum of laboratory spectra of methanol-rich ice mixtures at 10 K and the $3.47 \mu\text{m}$ feature from Reipurth 50. There is no contribution from a $3.47 \mu\text{m}$ feature in SVS 4-5. The contents of the laboratory mixtures are indicated in the lower panel.

is seen toward much fewer objects and is assigned to the ν_3 CH-stretching vibration band of solid methanol.

To estimate the true depth of the methanol band, it is necessary to remove the contribution from the $3.47 \mu\text{m}$ feature. A first-order approximation is to use a high signal-to-noise profile observed toward another YSO. We chose here the feature observed toward the intermediate mass YSO Reipurth 50 described in Dartois et al. (2003). The feature has a center position of $3.478 \mu\text{m}$ and a $FWHM$ of $0.12 \mu\text{m}$. $3.47 \mu\text{m}$ features from other sources give similar results (Brooke et al. 1999). The $3.47 \mu\text{m}$ band from Reipurth 50 was fitted to the observed spectra simultaneously with a laboratory methanol band.

It is well-known that the $3.53 \mu\text{m}$ methanol band is sensitive to the structure and composition of the ice (Ehrenfreund et al. 1999). Laboratory spectra are compared to the observed methanol bands in Fig. 3. A laboratory spectrum of pure methanol does not give a perfect fit of the exact profile to any of

Table 1. Column densities of solid methanol and water.

Source	$\tau(\text{H}_2\text{O})$	$N_{\text{H}_2\text{O}}^a$ 10^{18} cm^{-2}	$N_{\text{CH}_3\text{OH}}^a$ 10^{18} cm^{-2}	$N_{\text{CH}_3\text{OH}}/N_{\text{H}_2\text{O}}$
SVS 4-5	4 ± 1	7 ± 2	1.5 ± 0.1	0.21 ± 0.05
SVS 4-9	1.6 ± 0.1	2.5 ± 0.2	0.62 ± 0.05	0.25 ± 0.03
Cha I Na2	1.5 ± 0.1	2.2 ± 0.2	0.3 ± 0.05	0.14 ± 0.03

^a Statistical 1σ errors. Uncertain laboratory estimates of band strengths may introduce a systematic error of up to 30%.

the observed spectra, mainly due to the relative weakness of the secondary band of solid methanol at $3.40 \mu\text{m}$ in the observed spectra. It is interesting to note that the ratio of the $3.40 \mu\text{m}$ and the $3.53 \mu\text{m}$ methanol features in low-mass sources are similar to that of the high-mass sources of Dartois et al. (1999). A laboratory spectrum rich in water and formaldehyde (H_2CO) can reproduce the spectra. However, the H_2CO identification was found to be inconsistent for the massive stars W 33A and RAFGL 7009S (Dartois et al. 1999) due to the absence of bands at 5.8 and $6.69 \mu\text{m}$. Other mechanisms of reducing the strength of the $3.40 \mu\text{m}$ band cannot be ruled out. For example, irradiated pure methanol spectra annealed to temperatures higher than 60 K also gives good matches. For the estimate of the CH_3OH column densities it is assumed that H_2CO does not contribute to the $3.53 \mu\text{m}$ band.

The adopted band strength of the CH-stretching mode at $3.53 \mu\text{m}$ is $5.3 \times 10^{-18} \text{ cm molec}^{-1}$. This value is not found to vary significantly depending on the ice mixture (Kerkhof et al. 1999). The derived abundances are summarized in Table 1.

Brooke et al. (1999) and Chiar et al. (1996) find in general upper limits on the methanol abundance in the solid phase of a few % with respect to water. We find consistent results for the rest of our observed sample, i.e. methanol with an abundance of more than 5% is found toward only 3 out of a sample of ≈ 40 low mass YSOs.

3. Chemical implications

The methanol can be produced in space and in laboratory experiments through several different pathways. Gas-phase chemistry produces only low abundances of CH_3OH , of order 10^{-9} with respect to H_2 , so that simple freeze-out of gas-phase CH_3OH cannot reproduce the observed solid state abundances of $\sim 10^{-5}$. A possible route is therefore thought to be grain surface hydrogenation reactions of solid CO with atomic H, leading to H_2CO and eventually CH_3OH (Tielens & Hagen 1982; Charnley et al. 1997). Experimental results on

this reaction scheme at low temperatures are still controversial. Watanabe & Kouchi (2002) find efficient formation of H₂CO and CH₃OH by warm (≈ 300 K) hydrogen addition to CO in an H₂O-CO ice mixture, but the temperature of the hydrogen is not relevant for quiescent dark clouds. Other authors find yields which show that the formation of methanol directly via hydrogenation of CO is inefficient in dark clouds in the 10–25 K regime (Hiraoka et al. 2002). Further experiments are needed to solve this discrepancy.

Theoretical models of grain surface chemistry indicate that the fraction of CH₃OH ice with respect to H₂O ice, as well as the H₂CO/CH₃OH ratio, depend on the ratio of H accretion to CO accretion on the grains and thus on the density of the cloud (e.g., Charnley et al. 1997; Keane et al. 2002). In the framework of these models, solid CH₃OH abundances of 15–30% with respect to H₂O ice such as found here can only be produced at low densities, $n \approx 10^4$ cm⁻³. Moreover, the region needs to be cold, $T_{\text{dust}} < 20$ K, to retain sufficient CO on the grain surfaces. The models thus suggest that solid CH₃OH formation occurs primarily in the cold pre-stellar phase. However, this fails to explain the large range of methanol abundances observed along lines of sight toward low mass YSOs in the same star forming cloud, unless the duration of the pre-stellar phase varies strongly from source to source. As discussed by van der Tak et al. (2000), comparison of solid CH₃OH with solid CO₂ can further constrain the H/O ratio of the accreting gas and thus the density and duration of the pre-stellar phase. For low-mass YSOs, data on solid CO₂ are not yet available, but will be possible with the *Space Infrared Telescope Facility* (SIRTF) via the 15.2 μm CO₂ bending mode.

An alternative formation route of solid CH₃OH may be through ultraviolet processing (Schutte 1988) or proton irradiation of ices (Hudson & Moore 1999). However, as shown by van der Tak et al. (2000), the CH₃OH production rates in these experiments are orders of magnitude lower than those through grain surface formation. The fact that some low-mass sources show similarly high solid CH₃OH abundances as many massive sources argues further against ultraviolet radiation playing a significant role.

It is clear that any formation scheme of solid CH₃OH must be able to explain local ice mantle abundances of at least 15–30% compared to H₂O ice, regardless of the potential differences in density, temperature and ultraviolet radiation field between high- and low-mass YSO environments. At the same time, such models need to explain the large variations in solid CH₃OH abundances from object to object, with abundances of less than 3–5% found for both low- and high-mass YSOs (Chiar et al. 1996; Brooke et al. 1999). In this context, it is interesting that abundant solid methanol is now detected toward two sources which are members of the same dense cluster, SVS 4-5 and 4-9, while other nearby sources in Serpens such as CK 1 show solid methanol abundances of less than a few %. This suggests that the ice mantle chemistry may differ significantly between different regions even in the same star-forming clouds or that the formation and subsequent presence of methanol on grain surfaces is a transient phenomenon related to strong heating of the ices. In the last scheme the methanol may not exist for long in the solid phase before being desorbed by the

continuous heating of the ice. Finally shock processing may produce a different ice chemistry (Bergin et al. 1998). Making a survey of the SVS 4 cluster lines of sight may help to decipher the relation of the methanol ice to the environmental differences between “quiescent” environments as opposed to the massive and complex star-forming environments probed so far.

Acknowledgements. The authors wish to thank the VLT staff for assistance and advice, in particular Chris Lidman for many helpful comments on the data reduction. This research was supported by The Netherlands Organization for Scientific Research (NWO) grant 614.041.004, The Netherlands Research School for Astronomy (NOVA) and a NWO Spinoza grant.

References

- Bachiller, R., Liechti, S., Walmsley, C. M., & Colomer, F. 1995, *A&A*, 295, L51
- Bergin, E. A., Neufeld, D. A., & Melnick, G. J. 1998, *ApJ*, 499, 777
- Bernstein, M. P., Dworkin, J. P., Sandford, S. A., Cooper, G. W., & Allamandola, L. J. 2002, *Nature*, 416, 401
- Bernstein, M. P., Sandford, S. A., Allamandola, L. J., Chang, S., & Scharberg, M. A. 1995, *ApJ*, 454, 327
- Briggs, R., Ertem, G., Ferris, J. P., et al. 1992, *Origins of Life Evol. Biosphere*, 22, 287
- Brooke, T. Y., Sellgren, K., & Geballe, T. R. 1999, *ApJ*, 517, 883
- Carpenter, J. A., Hillenbrand, L. A., Skrutskie, M. F., & Meyer, M. R. 2002, *AJ*, 124, 1001
- Charnley, S. B., Tielens, A. G. G. M., & Millar, T. J. 1992, *ApJ*, 399, L71
- Chiar, J. E., Adamson, A. J., & Whittet, D. C. B. 1996, *ApJ*, 472, 665
- Dartois, E., Schutte, W., Geballe, T. R., et al. 1999, *A&A*, 342, L32
- Dartois, E., Thi, W.-F., Pontoppidan, K. M., et al. 2003, *A&A*, submitted
- Ehrenfreund, P., Kerkhof, O., Schutte, W. A., et al. 1999, *A&A*, 350, 240
- Eiroa, C., & Casali, M. M. 1989, *A&A*, 223, L17
- Eiroa, C., & Casali, M. M. 1992, *A&A*, 262, 468
- Gerakines, P. A., Schutte, W. A., Greenberg, J. M., & van Dishoeck, E. F. 1995, *A&A*, 296, 810
- Gibb, E. L. 2001, Ph.D. Thesis, Rensselaer Polytechnic Institute
- Giovannetti, P., Caux, E., Nadeau, D., & Monin, J.-L. 1998, *A&A*, 330, 990
- Hatchell, J., Thompson, M. A., Millar, T. J., & Macdonald, G. H. 1998, *A&AS*, 133, 29
- Hiraoka, K., Tesuya, S., Sato, S., et al. 2002, *ApJ*, 577, 265
- Hudson, R. L., & Moore, M. H. 1999, *Icarus*, 140, 451
- Kenyon, S. J., & Gómez, M. 2001, *AJ*, 121, 2673
- Kerkhof, O., Schutte, W. A., & Ehrenfreund, P. 1999, *A&A*, 346, 990
- Munõz Caro, G. M., Meierheinrich, U. J., Schutte, W. A., et al. 2002, *Nature*, 416, 403
- Persi, P., Marenzi, A. R., Kaas, A. A., et al. 1999, *AJ*, 117, 439
- Pontoppidan, K. M., Fraser, H., Dartois, E., et al. 2003, *A&A*, submitted
- Rodgers, S. D., & Charnley, S. B. 2001, *ApJ*, 546, 324
- Schöier, F. L., Jørgensen, J. K., van Dishoeck, E. F., & Blake, G. A. 2002, *A&A*, 390, 1001
- Schutte, W. A. 1988, Ph.D. Thesis, Leiden University
- van der Tak, F. F. S., van Dishoeck, E. F., & Caselli, P. 2000, *A&A*, 361, 327
- Watanabe, N., & Kouchi, A. 2002, *ApJ*, 571, L173